Characteristics of Ultradrawn Blend Films of Ethylene−Methyl Methacrylate Copolymer and Ultrahigh Molecular Weight Polyethylene Prepared by Gelation/Crystallization from Solutions Estimated by X-ray, Positron Annihilation, and ^{13}C NMR

Lin Ma,[†] Mama Azuma,[†] Chunqing He,[‡] Takenori Suzuki,[‡] Yuezhen Bin,[†] and Masaru Matsuo*,[†]

Textile and Apparel Science, Faculty of Human Life and Environment, Nara Women's University, Nara 630-8263, Japan, and Radiation Science Center of High Energy Accelerator Research Organization, 1-1 Oho, Tsukuba, Ibaraki 305-0801, Japan

Received December 12, 2003

ABSTRACT: Copolymer ethylene−methyl methacrylate (EMMA) and ultrahigh molecular weight polyethylene (UHMWPE) were blended in decalin solvent. Two kinds of EMMA films with different contents of the MMA side group were used as test specimens. A hot homogenized solution was poured into an aluminum tray to form gels, and the decalin was allowed to evaporate from the resultant gels under ambient condition. Surprisingly, the resultant dry blend films could be elongated up to more than 200-fold ($\lambda = 200$) at 135 °C. Such a great draw ratio could be realized even for a blend film with 90% EMMA content (the 9/1 film), although the maximum draw ratio of EMMA homopolymer films was 10-fold ($\lambda = 10$). The greatest drawability for the 9/1 films was attributed to large crystal lamellae of UHMWPE, ensuring a crystal transition from a folded to a fibrous type. Accordingly, EMMA chains were independent of the ultradrawing of UHMWPE and kept a random orientation under the ultradrawing process. The storage (Young's) moduli were 20−25 GPa at 20 °C. In contrast, EMMA chains within the 1/1 films were oriented drastically together with UHMWPE crystallites. The moduli of the 1/1 films at 20 °C reached 75−85 GPa, which are close to 100 GPa of UHMWPE homopolymer films with $\lambda = 100$ and are higher than the value (40 GPa) of polypropylene films with $\lambda = 100$ as well as the crystal lattice modulus (41−43 GPa) along the chain direction. The morphology of the blend films with such different orientation modes of EMMA chains was analyzed by using X-ray, ^{13}C NMR, and positron annihilation. As a result, the drastic orientation of EMMA chains within the 1/1 film was thought to be due to the epitaxial nucleation surface for ethylene sequences of EMMA under the cooling process from 135 °C to room temperature after the elongation. However, the amount of EMMA content within the 9/1 film was obviously too much to develop the epitaxial nucleation surface effect. Even so, it was confirmed that most of the highly oriented ethylene sequences of EMMA within the 1/1 film exist as an amorphous phase, causing the β (mechanical) dispersion associated with a large (macro-Brownian) movement.

Introduction

In previous papers,[1,2] the effect of side groups on the crystallization of ethylene main chains was investigated by using copolymer ethylene−methyl methacrylate (EMMA). The result revealed that the longer ethylene sequences in the noncrystalline phase had a nonrandom local arrangement, but the bulky volume of the MMA side groups suppresses the crystallization of ethylene sequences. Consequently, even though crystallization is suppressed, the tendency for longer ethylene sequences to self-order leads to a dynamic local ordering in the noncrystalline phase. Furthermore, low crystallinity of EMMA films drawn up to their maximum draw ratio ($\lambda = 10$) caused a drastic shrinkage as well as drastic stress relaxation by chain slippage under a constant strain at room temperature.

To ensure dimensional stability of the drawn EMMA films, how to obtain stable crystallization of the ethylene sequences of EMMA is one of the important factors. As one of trials, EMMA and ultrahigh molecular weight polyethylene (UHMWPE) blends were prepared by gelation/crystallization from dilute solutions. Surprisingly, the elongation of the blend film (the 9/1 film) with 90% EMMA reached 300-fold ($\lambda = 300$), while the maximum draw ratio of the 1/1 film was 200-fold. For ultradrawn 9/1 and 1/1 films, no shrinkage occurred at room temperature for the drawn blends.

Certainly, it is well-known that the ultradrawing of UHMWPE has attracted much attention due to interest in producing high strength and high modulus fiber commercially. The gel-spun UHMWPE fibers exhibit excellent mechanical properties with a Young's modulus of 100−220 GPa and a tensile strength of 3−6 GPa.[3−7] Such mechanical properties are ascribed to the highly oriented and fully extended chains with respect to the stretching direction. However, the poor dyeing property and poor lamination of ultradrawn polyethylene films are big problems to expand the utility at the commercial level, although there has been several successful reports for dyeing of low molecular weight polyethylene (LMWPE) and polypropylene films by using supercritical fluids such as CO_2 or N_2O by Knittel et al.[8] and Bach et al.[9] Ultradrawing of blending polyethylene with other polymers having polar groups is one of the possible strategies for overcoming this problem. Unfortunately,

[†] Nara Women's University.
[‡] Radiation Science Center of High Energy Accelerator Research Organization.
* To whom all correspondence should be addressed: Fax 81-742-20-3462; e-mail m-matsuo@cc.nara-un.ac.jp.

10.1021/ma0305840 CCC: $27.50
Published on Web 09/03/2004

Table 1. Characterization of EMMA and UHMWPE Films

specimen	MMA, mol %	max draw ratio	mp, °C	$\bar{M}_v$[a]	$\bar{M}_n$[b]
EMMA-II(WH202)	6.5	6	85		4.3×10^4
EMMA-III(WM403)	14.6	10	64		3.1×10^4
UHMWPE		300	142	6.0×10^6	

[a] M_v = average viscosity molecular weight. [b] M_n = average number molecular weight.

no successful representation of high modulus and high strength fibers and/or films has been achieved for the blends of UHMWPE and other polymers, except for the polyethylene/polypropylene blend system.[10,11]

This paper is concerned with the morphology and mechanical properties of ultradrawn blend films of UHMWPE and EMMA having polar groups in order to study the origin of the greatest drawability and excellent thermal dimensional stability. The analysis is done mainly by using X-ray, ^{13}C NMR, and positron annihilation. The focus is concentrated on two points. One is the cocrystallization of ethylene sequences between EMMA and UHMWPE, leading to an epitaxial nucleation surface for ethylene sequences of EMMA under elongation. The other is the property of an extended amorphous ethylene sequence. The latter purpose is due to the fact that the investigation for highly oriented amorphous ethylene sequence is very difficult because of difficulty in preparing drawn amorphous polyethylene films. Incidentally, we must emphasize that the preliminary experiments were carried out for various EMMA/UHMWPE compositions between 9/1 and 1/1 at various draw ratios (λ) of between 1 and 100. The obtained results, however, provided middle values between the indicated compositions as well as between the indicated draw ratios. Accordingly, among the obtained results, the results for the indicated two compositions at $\lambda = 1$ and 100 are adopted to shorten the present paper.

Experimental Section

The materials used in the present work were EMMA and UHMWPE. Among three kinds of EMMA used in the previous paper,[1] two EMMA samples, EMMA-II and EMMA-III with higher contents of the MMA side group, were adopted as test specimens. The detailed characteristics of the two specimens were described elasewhere.[1,2] UHMWPE (Hercules 1900/90189) has an average viscosity molecular weight ($\bar{M}_v$) of 6×10^6. The structural characteristics of EMMA-II, EMMA-III, and UHMWPE are listed briefly again in Table 1. In preparing the blend samples by gelation/crystallization, the concentration of UHMWPE was fixed to be 0.4 g/100 mL against the solvent. The solvent was decalin. The chosen 0.4 g/100 mL was the optimum concentration of the UHMWPE solutions to prepare high modulus and high strength films.[7] The amount of EMMA was determined relative to that of the UHMWPE, in which the 9/1 and 1/1 compositions of EMMA and UHMWPE correspond to (3.6 g(EMMA) + 0.4 g(UHMWPE))/100 mL and (0.4 g(EMMA) + 0.4 g(UHMWPE))/100 mL, respectively.

The solution was prepared by heating a well-blended polymer/solvent mixture at 135 °C for 20 min under nitrogen. The homogenized solution was quenched to room temperature by pouring it into an aluminum tray ($10 \times 10 \times 10$ cm^3), thus generating a gel. The amount of solution in the tray was controlled to obtain the same thickness of samples, independent of the concentration of the solution. The decalin was allowed to evaporate from the gels under ambient conditions. The resulting dry gel film was vacuum-dried for 1 day to remove any residual trace of decalin. After then, the specimens were elongated manually up to the desired draw ratios at 135 °C under nitrogen and cooled to room temperature. The elongation-to-draw ratio beyond $\lambda = 20$ was done in a second stage because of the physical restriction of the size of the oven. Thus, the original specimen, the length being 10 mm, was first drawn to $\lambda = 20$, and the drawn film was cut into strips of length 50−60 mm. The specimens, each clamped over a length (30−40 mm) at the end, were drawn to the desired draw ratio beyond $\lambda = 20$ in a second stage.

In preliminary experiments, solvent cast films of EMMA-II and EMMA-III homopolymers were prepared, but all of the characteristics of the resultant films were confirmed to be perfectly equal to those of their melt films described in a previous paper.[1]

X-ray. X-ray measurements were carried out with a 12 kW rotating-anode X-ray generator (Rigaku RAD-rA). An X-ray beam by Cu Kα radiation at 200 mA and 40 kV was monochromatized with a curved graphite monochromator. The wide-angle X-ray diffraction (WAXD) intensity distribution was obtained at the desired temperatures from −110 to 60 °C by using a curved position-sensitive proportional counter (PSPC). To pursue the exact measurement of the diffraction intensity, the accumulated time was set to be 30 min at each temperature. The small-angle X-ray scattering (SAXS) intensity distribution was measured as a function of the scattering angle ($2\theta_B$) in the meridional direction by the PSPC system.

^{13}C NMR. NMR measurements as a function of the temperature were carried out for the EMMA melt films on a JEOL JM-EX 270 spectrometer, operating at 67.8 MHz for ^{13}C. The measurements for ^{13}C CP (cross-polarization)/MAS as well as ^{13}C PST (pulse saturation transfer)/MAS were performed at room temperature. The actual temperatures in the probe under spinning were confirmed to be in the range of 27−36 °C. The chemical shifts were determined relative to the higher field signal (29.5 ppm) of adamantane. The detailed conditions are described elsewhere.[2]

Positron Annihilation. Positron annihilation experiments were conducted with a conventional fast−fast coincidence system having a time resolution of 300 ps full width at half-maximum (fwhm).[2] The time spectrometer was composed of two plastic scintillation detectors (40 mm diameter × 40 mm Pilot-U mounted on a Hamamatsu H1949 photomultiplier), two differential constant fraction discriminators (ORTEC 583) (one for start signals from 1.28 MeV γ-rays and the other one for stop signals from 0.511 MeV annihilation γ-rays), a time-to-amplitude converter (ORTEC 4570), and a multichannel analyzer with a 1024 conversion gain (O921). The accumulated data were controlled by a personal computer (Dell PC).

A position source was prepared by depositing ca. 1.1 MBq (30 μCi) of aqueous $^{22}NaCl$ on a Kapton foil of 7 μm thickness and 10 × 10 mm area. After drying, the foil was covered with the same size of the foil, and the edges were glued with epoxy resin. The source was further sealed in a 3 μm Mylar foil and then sandwiched by two identical samples for positron annihilation measurements. The diameter of the spot of the ^{22}Na source was ca. 2 mm. During the measurement, the samples were kept in a vacuum cell, in which the temperature of the samples was controlled. Spectra were recorded every hour, and about 1−2 million events were stored in each spectrum.

As described in a previous paper,[2] positrons emitted from ^{22}Na induce a radiation effect on polymer samples, and electrons are excited from the constituent atoms. After these positrons with an average energy of 200 keV lose their energies through interacting with atoms and molecules, they are finally thermalized and capture the excited electrons to form positroniums (Ps, hydrogen-like atom consisting of e^+ and e^-). There are two Ps states: para-Ps (p-Ps) and ortho-Ps (o-Ps). Although the former annihilates within 125 ps, the latter can last for 140 ns in a vacuum. o-Ps can migrate in a polymer and tends to be trapped in intermolecular spaces, in which o-Ps can pick off electrons from the surrounding atoms and annihilate with a shorter lifetime than that of the annihilation in a vacuum.

Viscoelastic Measurements. The complex dynamic tensile modulus was measured at 10 Hz over the temperature range from −150 to 150 °C by using a viscoelastic spectrometer (VES-F) obtained from Iwamoto Machine Co. Ltd. The length

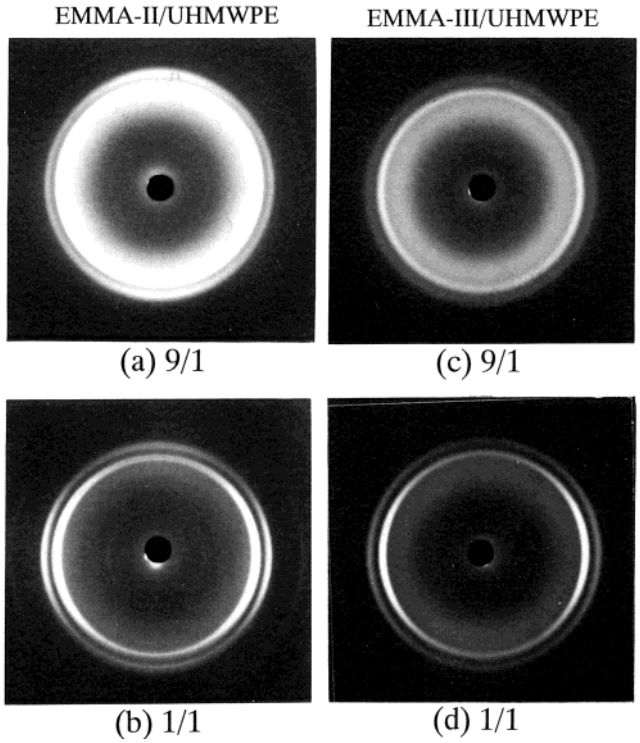

Figure 1. WAXD patterns (end view) for the EMMA/UHMWPE blend films (9/1, 1/1) with $\lambda = 1$.

of the specimen between the jaws was 40 mm, and the width was about 1.5 mm. The complex dynamic modulus was measured by imposing a small dynamic strain to ensure a linear viscoelastic behavior of the specimen.[12] In doing so, the specimen was subjected to a static tensile strain in the range 0.05−0.1% to place the sample in tension during the axial sinusoidal oscillation.

DSC Measurements. Calorimetric investigations of EMMA and their blends were performed with an Exstar 6000 of Seiko Instrument Inc. The heating rate was 1 °C/min. The weight of the specimen was 10 mg.

Results and Discussion

Figure 1 shows the WAXD patterns observed from undrawn blend films. An X-ray beam was directed parallel to the film surface. The characteristic diffractions from the (110) and (200) planes for the 1/1 film indicate the preferential orientation of the *c*-axis perpendicular to the film surface, which is similar to the diffraction intensity from single-crystal mats, reported by Smith et al.[5] On the other hand, the diffraction rings for the pattern of the 9/1 films indicate a random orientation of crystallites. As described in the previous papers, the crystal unit of EMMA was similar to an orthorhombic form of the polyethylene crystal unit, and then the diffraction peak positions of EMMA were almost the same as the peak position of polyethylene. Accordingly, the diffraction rings in Figure 2 are thought to be due to only the contribution from UHMWPE, since the crystallinity of EMMA is much lower than that of UHMWPE.

Figure 2 shows the SAXS intensity distributions (end view) of undrawn blends and individual homopolymers (EMMA-II, EMMA-III, and UHMWPE). The intensity distribution from the blend films shows scattering maxima corresponding to long periods. The values are listed in Table 2. With increasing the EMMA contents, the long period became shorter. As shown in Figure 2, the scattering maxima became less distinct as the

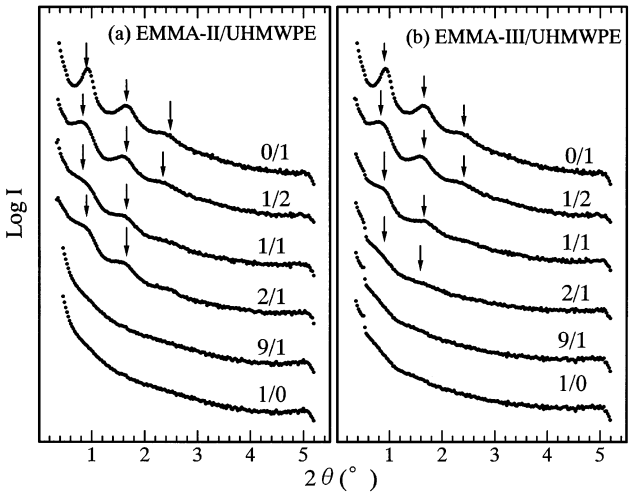

Figure 2. SAXS intensity distributions for the EMMA/UHMWPE blend film in the meridional direction.

Table 2. Long Period *L* of Blend Films with Different Compositions

L (Å)	0/1	1/2	1/1	2/1	9/1
EMMA-II/UHMWPE	111.5	110.4	109.1	108.3	–
EMMA-III/UHMWPE	111.5	110.2	109.1	108.4	–

EMMA content increased. The SAXS distributions and WAXD patterns together indicate that the 1/2 and 1/1 films were composed of highly oriented crystal lamellae with their flat face parallel to the film surface, like UHMWPE (0/1). The UHMWPE crystal lamellae were oriented with their flat faces parallel to the film surface in evaporation process of solvent. This is reasonable since such orientation of crystal lamellae is common sense to be stable energetically. In contrast, the orientation fluctuation of crystal lamellae became more pronounced with increasing EMMA content. The profile of the intensity distribution from the 9/1 film shows a monotonic curve. The scattering peaks of the EMMA-III/UHMWPE blends with the same composition have almost the same profile as those of the corresponding EMMA-II/UHMWPE blends. Here, it may be expected that the isolated UHMWPE chains within the 9/1 film also form large crystal lamellae of UHMWPE under gelation, but the crystal lamellae cannot orient parallel to the film surface. This is thought to be due to the fact that large amounts of EMMA hamper the ordered orientation of the lamellae of UHMWPE. Incidentally, the continuous change in the peak height provided the middle values between the 9/1 and 1/1 composites as well as between draw ratios at $\lambda = 1$ and 100. Accordingly, as described in Introduction, the following discussions were made for the 9/1 and 1/1 films at $\lambda = 1$ and 100.

Figure 3 shows WAXD patterns for the 9/1 and 1/1 films drawn up to $\lambda = 100$. The profiles of WAXD were confirmed to be almost the same for specimens with $\lambda = 50-200$. Accordingly, the following discussion was only made for the specimens with $\lambda = 100$. The patterns observed for the 9/1 film indicate different orientation modes between EMMA and UHMWPE crystallites. That is, the weak diffraction rings from the (110) and (200) planes are reflections from EMMA crystallites with a random orientation, while the sharp diffraction spots are due to highly oriented UHMWPE crystallites with respect to the stretching direction. On the other hand, the pattern of the 1/1 film shows sharp diffraction spots

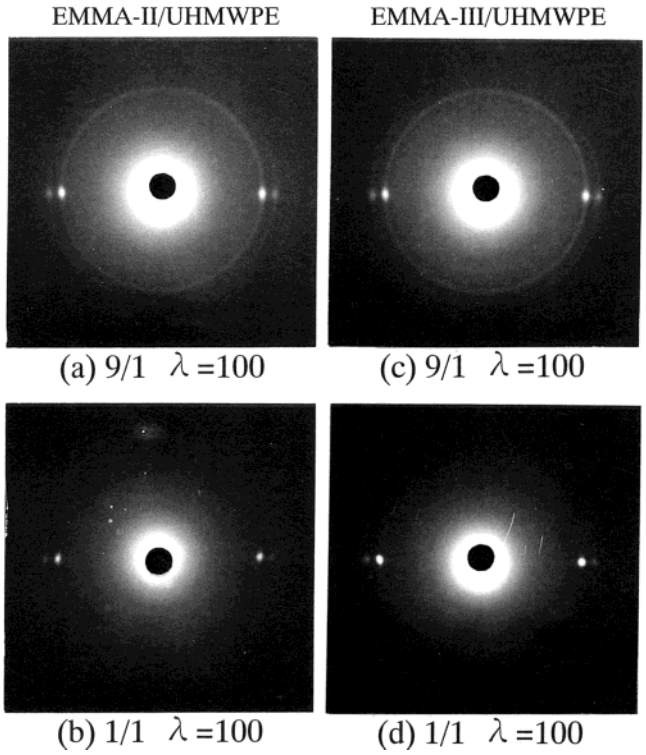

Figure 3. WAXD patterns (through view) for the EMMA/UHMWPE blend films (9/1, 1/1) with $\lambda = 100$.

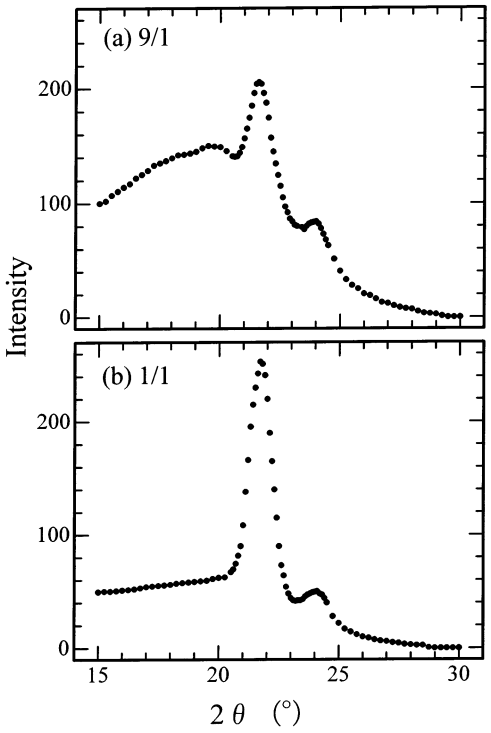

Figure 4. WAXD intensity distributions of the 9/1 and 1/1 compositions of the EMMA-III/UHMWPE blend film with $\lambda = 100$. Specimens were rotated 60 times/min around the film normal direction.

from the (110) and (200) planes, and no ring appears, indicating that EMMA and UHMWPE crystallites are predominantly oriented together in the stretching direction. Such orientation modes dependent upn EMMA content, as observed for UHMWPE/LMWPE blend films already,[13] are thought to be due to their different crystallization modes under the elongation process.

Figure 4 shows the WAXD intensity distribution of the 9/1 and 1/1 films for EMMA-III and UHMWPE with $\lambda = 100$. The film thickness between the 9/1 and 1/1 films was almost the same, ca. 15 μm. The measurements were made using a special attachment set in the X-ray instrument. The drawn specimen was rotated 60 times/min around the film normal direction to obtain the average diffraction intensity for the drawn films. The scanning speed of the detector of the diffraction beam was to be 100 s for 0. 1° (twice the Bragg angle $2\theta_B$) to ensure a sufficient accumulation time at each $2\theta_B$. This method played an important role to estimate the crystallinity of the film by X-rays. In addition to the (110) and (200) planes, a very broad peak at around 19.2°, observed for the 9/1 film, corresponds to an amorphous peak from EMMA-III, while no amorphous peak was observed for the 1/1 film, indicating the oriented crystallization of the EMMA-III chains. This means that the orientation and crystallization of the EMMA chains within the drawn 1/1 film are quite different from those of the EMMA chains within the drawn 9/1 film.

To pursue a more quantitative analysis, the temperature dependence of the diffraction intensity was measured by a curved PSPC in the range from −130 to 135 °C. Figure 5 shows the results for EMMA-III and UHMWPE blend films with $\lambda = 100$ and the corresponding UHMWPE homopolymer film. The measurements were carried out only in the horizontal direction, since the special instrument used in Figure 4 could not be used for the measurements at elevated temperature. All of the specimens were maintained for 10 min at the indicated temperatures before measurements, and the accumulation of the intensity was made for 30 min. In this case, for the 9/1 film, no peak can be observed at around 19.2° (see Figure 4) because of a large sharp diffraction peak from the (110) plane of UHMWPE crystallites oriented perfectly with respect to the stretching direction. Accordingly, it was impossible to judge whether most of the oriented EMMA-III chains form the amorphous state with a highly ordered arrangement with respect to the stretching direction. As described before, the two peaks correspond to the overlapped reflections concerning the (110) and (200) planes of EMMA-III and UHMWPE with an orthorhombic crystal unit. The large peak shift of the (200) plane to a lower angle with increasing temperature is due to thermal expansion of the *a*-axis. This tendency is most considerable for the 9/1 blend film reflecting the unstable state of EMMA-III crystallites. The overlapped peaks concerning the (110) and (200) planes become less intense with increasing temperature, indicating a partial melt of the EMMA crystallites. The EMMA crystallites within the 9/1 film take a random orientation as shown in Figure 3c, and the melting point of EMMA crystallites was close to that of EMMA homopolymer crystallites prepared by a melting press.[1] In contrast, for the 1/1 film, the peak intensity is almost independent of the temperature. This tendency is almost similar to the temperature dependence of UHMWPE homopolymer, indicating that cocrystallites of EMMA and UHMWPE within the 1/1 film are stable like UHMWPE crystallites. Such considerably different temperature dependence, relating to different EMMA contents, is due to the fact that the crystallization mode of the ethylene sequences is sensitive to the EMMA content within the blend. Namely, as shown in Figure 3d, the EMMA and

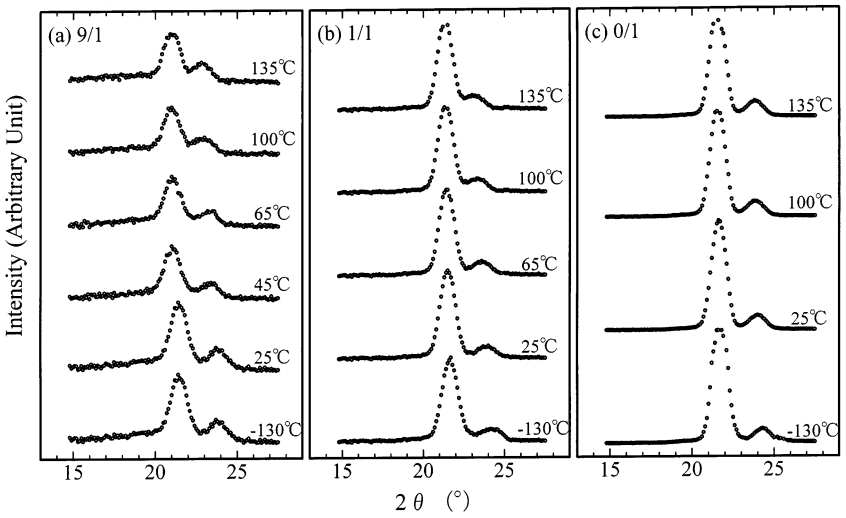

Figure 5. WAXD intensity distributions for the EMMA-III/UHMWPE blend gel films, which were drawn to 100 times at elevated temperatures.

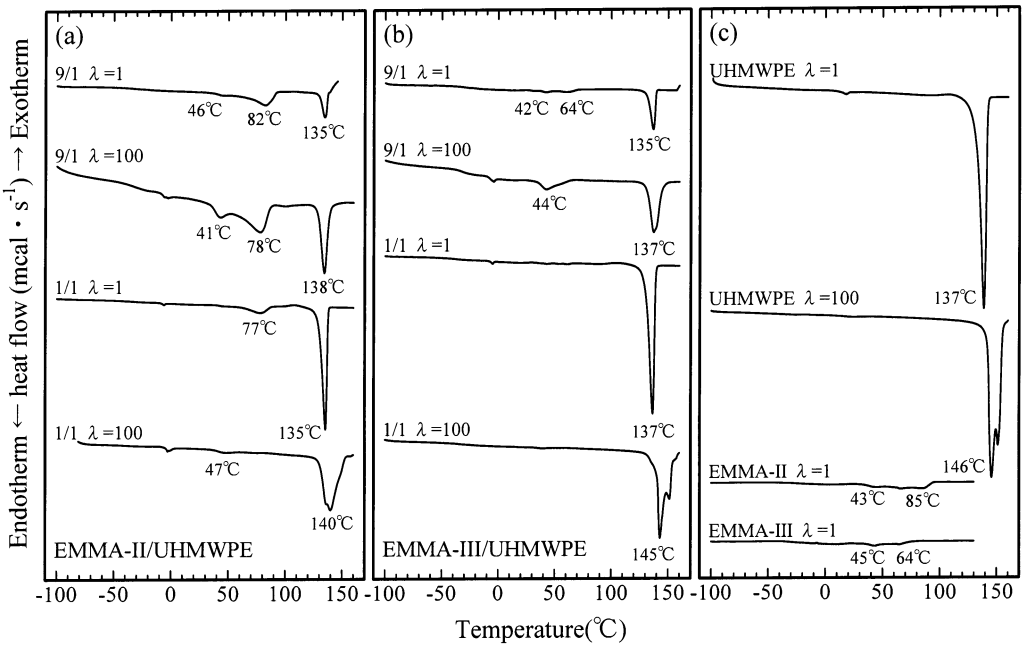

Figure 6. DSC curves for (a) EMMA-II/UHMWPE, (b) EMMA-III/UHMWPE, and (c) UHMWPE, EMMA-II, EMMA-III films at the indicated draw ratios.

UHMWPE crystallites within the 1/1 film are oriented together drastically in the stretching direction, and furthermore the temperature dependence of X-ray intensity distributions of the 1/1 film and UHMWPE homopolymer film in Figure 5b,c suggests that the melting point of the oriented EMMA crystallites is almost equal to that of the oriented UHMWPE crystallites. To analyze the different oriented crystallization modes, DSC measurements were made for the 9/1 and 1/1 films.

Parts a and b of Figure 6 show the DSC curves for EMMA-II and UHMWPE blend films and EMMA-III and UHMWPE blend films, respectively, measured at $\lambda = 1$ and 100. Figure 6c shows the DSC curves of UHMWPE films with $\lambda = 1$ and 100 as well as EMMA-II and EMMA-III films with $\lambda = 1$. In the measurements, dry films weighing 10 mg were placed in a standard aluminum sample pan. The amount of UHMWPE within the 9/1 film was about 20% against that within the 1/1 film. As shown in column (a), the three peaks of EMMA-II for the 9/1 film appearing at temperatures <82 °C show clear profiles at $\lambda = 1$ and 100. In contrast, the peak of EMMA-II for the 1/1 film is much smaller than that for the 9/1 film. Judging from the curves of UHMWPE in Figure 6c, it is evident that the peak position of UHMWPE within the blend film at $\lambda = 100$ shifts to the lower temperature side compared with the melting peak of the UHMWPE homopolymer. This indicates that the large amount of EMMA chains suppresses the crystal growth of UHMWPE due to oriented crystallization under elongation, although the orientation of UHMWPE crystallites within the 9/1 and 1/1 films are confirmed to be almost the same as that within UHMWPE homopolymer film. It may be noted that for the 1/1 film the small peak of EMMA-II ($\lambda = 1$) at 77 °C disappears by elongation up to $\lambda = 100$, and

the peak of UHMWPE is broader. The peak at $\lambda = 100$ is at the lower temperature side than the peak of the UHMWPE homopolymer film. These results indicate the cocrystallization of EMMA and UHMWPE chains under elongation and cooling processes. If cocrystallization of EMMA and UHMWPE chains within the 1/1 film did not occur under elongation, the large peak must appear at the same temperature (146 °C) as observed for the UHMWPE film, reflecting only the melting of UHMWPE crystallites. On the basis of the melting point of EMMA being much lower than that of UHMWPE, the mechanism of cocrystallization under elongation is thought to be due to an epitaxial nucleation surface for ethylene sequences of oriented EMMA chains under the cooling process to room temperature after elongation. Namely, the ethylene sequences of melted EMMA chains are oriented by the shear stress leading to the orientation of UHMWPE chains with respect to the stretching direction, and they promote the growth of crystallites on the surface of extended crystal chains of UHMWPE under the cooling process.

It may be expected that the epitaxial growth of EMMA occurs easily since the crystallization part of EMMA is ethylene sequences like polyethylene. For the 9/1 film, very few EMMA chains adjacent to UHMWPE crystallites are probably thought to be oriented predominantly together with UHMWPE crystallites by the shear stress, but most of the remaining EMMA chains maintained a random orientation and crystallized separately, since the amount of EMMA was 90% against that of UHMWPE.

As for the EMMA-III and UHMWPE blends, the peak magnitude of EMMA-III at the lower temperature side was very weak even for the 9/1 film because of the crystallinity of EMMA-III chains lower than that of EMMA-II (see Figure 6b). The peak shift of UHMWPE by elongation up to $\lambda = 100$ is only 2 °C, and the peak position of the elongated film is lower than that of the UHMWPE homopolymer, indicating that the large number of EMMA-III chains suppresses the crystal growth of UHMWPE under oriented crystallization. As for the 1/1 film, no peak of EMMA-III was observed, reflecting unstable crystallites with large fluctuation of crystal lattice distance. The existence of such unstable crystallites cannot be confirmed by DSC measurement, despite the appearance of the very weak but observable diffraction rings by X-ray measurement (see Figure 3a,b).

Figure 7 shows the 67.8 MHz CP (cross-polarization)/MAS and PST (pulse saturation transfer)/MAS ^{13}C NMR spectra of the 9/1 and 1/1 films (EMMA-III/UHMWPE) with $\lambda = 1$ and $\lambda = 100$ at room temperature. As described in a previous paper,[1] the CP/MAS spectra show two peaks with chemical shifts of 32.8 ppm (peak I) and 30.8 ppm (peak II), which can be assigned to the orthorhombic crystalline and noncystalline methylene carbons in the ethylene sequence, respectively. The assignment of the other peaks was made according to the DD/MAS spectra of ethylene (dimethylamino)ethyl (EDAM), reported already,[1] as well as the solution NMR spectra.[14] All of the spectra were analyzed on the basis of the assumption of a superposition curve of Gaussian and Lorentzian functions. In this process, the line width and the peak height of each component were determined to give the best fit by computer based on the small changes from the initial peak position. The initial values of the all components were given by adopting the

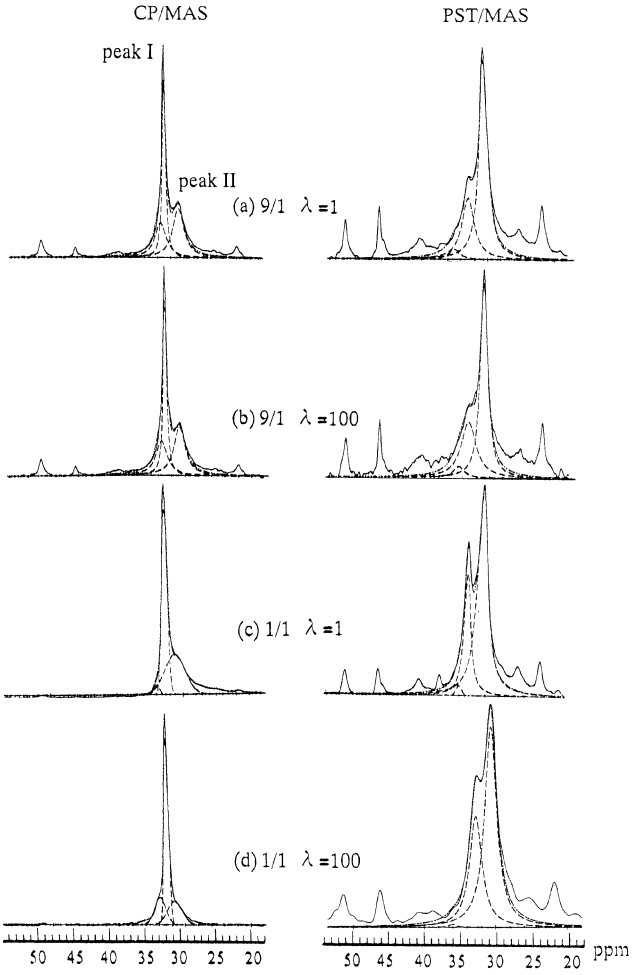

Figure 7. 67.8 MHz ^{13}C CP/MAS and PST/MAS spectra measured for the EMMA-III/UHMWPE (9/1, 1/1) at the indicated draw ratios.

corresponding chemical shifts of EMMA and UHMWPE obtained elsewhere.[14,15] The spectrum indicates the existence of an orthorhombic crystal (O), a monoclinic crystal (M), and rubbery (R) components.[16−18]

As shown in this figure, the existence of an interfacial component cannot be observed for the blend films despite the appearance for the EMMA-III homopolymer.[1] For semicrystalline polymers, the CP/MAS spectra emphasize the contribution of the crystalline phase, while the PST/MAS spectra acquired with a short repetition time emphasize the contribution of the amorphous phase. Considering the ^{13}C NMR CP/MAS spectrum of the EMMA-III homopolymer with $\lambda = 1$, reported in a previous paper,[1] peak I of the CP/MAS spectrum for the 9/1 film with $\lambda = 1$ is attributed mostly to the orthorhombic crystalline signal (O) of UHMWPE, while peak II is the rubbery signal (R) of the noncrystalline phase of EMMA-III. Here, the CP/MAS and PST/MAS spectra for the 9/1 film provide almost the same profiles of peak I and peak II for the 9/1 films, which are independent of the draw ratio. This indicates that elongation up to $\lambda = 100$ causes no significant effect on the local ordering and the oriented crystallization of ethylene sequences in the amorphous region of EMMA-III by elongation. This result is in good agreement with a random orientation of EMMA crystallites observed for the WAXD pattern in Figure 3c. Namely, if the significant oriented crystallization of EMMA with the 9/1 blend occurred under the elongation, the amorphous

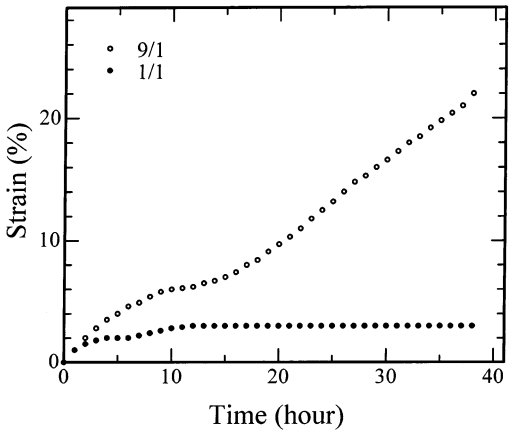

Figure 8. Changes in strain against time for the EMMA-III/UHMWPE blends (9/1,1/1) with $\lambda = 100$ under a constant stress of 20 MPa.

content must be fewer. In such a condition, peak II of the PST/MAS at $\lambda = 100$ must be smaller than that at $\lambda = 1$, while peak I of the CP/MAS at $\lambda = 100$ must be larger than that at $\lambda = 1$. Both the actual curves, however, maintain the similar profiles, independent of the draw ratio. On the other hand, peak II of the CP/MAS spectrum for the 1/1 film decreases for the drawn films, while peak I of PST/MAS is independent of the elongation. This indicates that a slight increase in the crystallinity is produced by oriented crystallization, but most of the highly oriented ethylene sequences of EMMA are maintained as extended amorphous chains. This is discussed later in detail.

Figure 8 shows changes in the strain as a function of time for the 9/1 and 1/1 films (EMMA-III/UHMWPE) with $\lambda = 100$, when a constant stress of 20 MPa is applied as an external excitation. This creep experiment at 20 °C was carried out to support a series of experimental results by X-ray, DSC, and ^{13}C NMR. It can be seen that the strain for the 9/1 film increases with time, while a very small increase in the strain is observed for the 1/1 film. This means that partly oriented EMMA-III chains within the 9/1 film undergo drastic molecular slippage because of very few entanglements between the EMMA-III and UHMWPE amorphous chain segments. In contrast, it may be expected that the highly oriented EMMA-III chains within the 1/1 film are maintained without slippage by disentanglements, which reflect the crystallization of some ethylene sequences of EMMA-III, leading to an epitaxial nucleation surface for ethylene sequences of EMMA.

Figure 9 shows the temperature dependence of the storage modulus (E') and the loss modulus (E'') of EMMA-II/UHMWPE blends at a frequency of 10 Hz. The measurements were performed for the 9/1 and 1/1 films and UHMWPE homopolymer (0/1) films with $\lambda = 1$ and 100. Figure 10 shows the results of EMMA-III/UHMWPE blends. As shown in Figures 9 and 10, the 1/1 films with $\lambda = 100$ provide large values of E' beyond 75 GPa at 20 °C, which are slightly lower than the value (100 GPa) of E' for the corresponding UHMWPE but higher than the value (40 GPa) of ultradrawn polypropylene ($\lambda = 100$)[19] as well as the crystal lattice modulus (41−43 GPa) along the chain direction.[20] In contrast, the values of E' of the 9/1 films with $\lambda = 100$ are about 20−25 GPa, which are much lower than those (75 GPa) of the 1/1 film. This is obviously due to the fact that the EMMA chains within the 9/1 films take a random

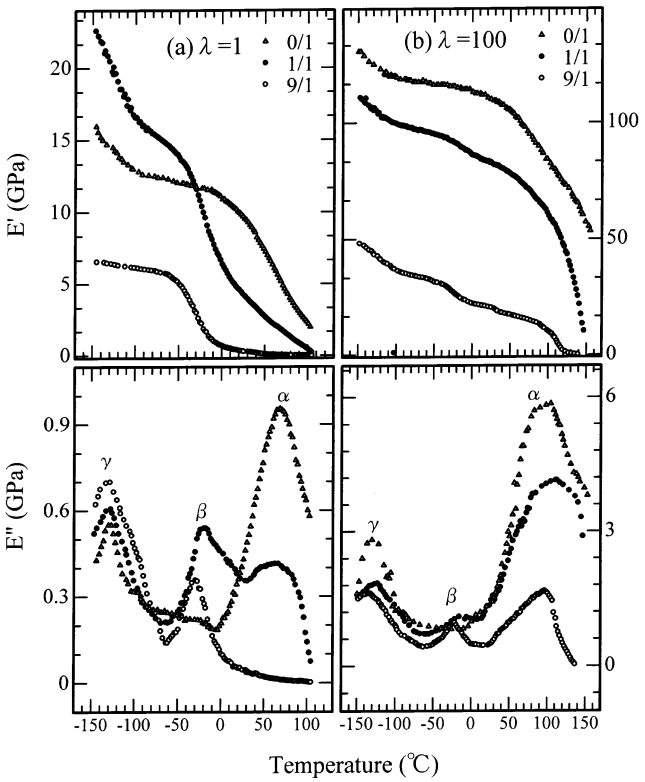

Figure 9. Temperature dependence of the storage and loss moduli for the EMMA-II/UHMWPE blend films and the UHMWPE film at the indicated draw ratios.

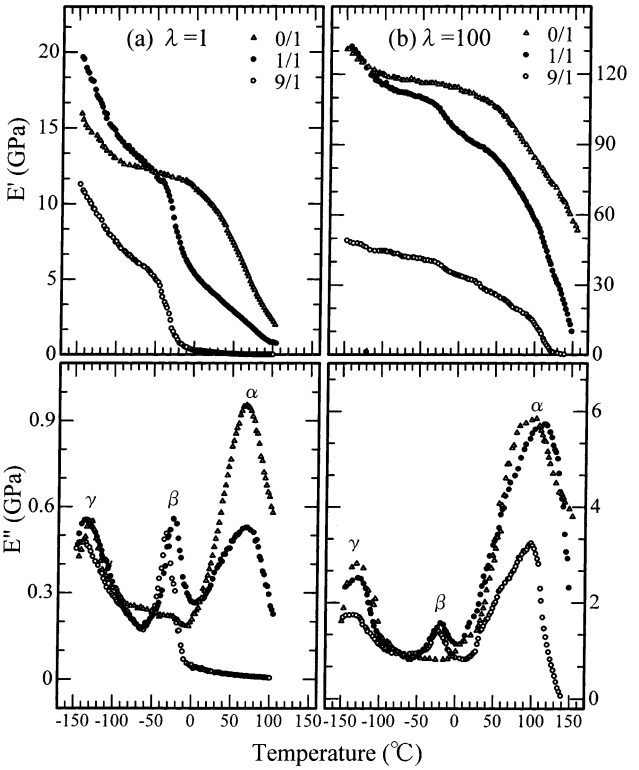

Figure 10. Temperature dependence of the storage and loss moduli for the EMMA-III/UHMWPE blend films and the UHMWPE film at the indicated draw ratios.

orientation, while those within the 1/1 films orient predominantly with respect to the stretching direction together with UHMWPE crystallites (see Figure 3).

The temperature dependence of E'' is sensitive to the introduction of EMMA. For the 1/1 films, three disper-

sion peaks (α, β, and γ relaxations) are observed.[21] The α relaxation is essentially associated with crystal dispersion.[22] The α relaxation discussed in this paper is related to cocrystallites of UHMWPE and EMMA. No α relaxation peak was observed for the 9/1 films with $\lambda = 1$ because of very few amounts of UHMWPE crystallites; the appearance of the α dispersion at $\lambda = 100$ is due to the growth of crystallization of UHMWPE by elongation. On the other hand, the α relaxation for the 1/1 undrawn films can be clearly observed because of a large number of UHMWPE crystallites. The increase in the magnitude with elongation is due to an increase in the crystallinity of UHMWPE as well as the crystallization of EMMA chains due to an effect of the epitaxial nucleation surface of the ethylene sequence of EMMA. The β relaxation appears at around −25 °C. Here, we must emphasize that the β relaxation cannot be assigned as a glassy transition. In accordance with Arrhenius plots in the previous paper,[2] the activation energies of EMMA-II and EMMA-III were 146 and 139 kJ/mol, respectively, which are higher than the values (114−115 kJ/mol) obtained for branched polyethylene (G201 and G808).[2] Accordingly, it was concluded that, together with positron annihilation measurements, the β relaxation of polyethylene is generally associated with a large motion of amorphous chains. Judging from a very small peak concerning the β relaxation of undrawn UHMWPE homopolymer film, the β relaxation is mainly attributed to the contribution from the large motion of amorphous EMMA chains.[2] The β relaxation peak magnitude becomes lower with the draw ratio λ. However, the peak can also be observed for the blend film with $\lambda = 100$. This means that under elongation the MMA side groups suppress the crystallization of ethylene sequences of EMMA, even when the EMMA chains within the 1/1 film are oriented predominantly with respect to the stretching direction. Namely, most of the oriented EMMA chains exist as an amorphous state with a highly ordered arrangement and/or unstable crystallites with large fluctuation of the lattice distance. This supports the X-ray results in Figures 4 and 5 as well as ^{13}C NMR spectra in Figure 7. The highly oriented amorphous chains of EMMA cause the partial crystallization of ethylene sequences, and the resultant small crystallites play the role of junction points. This result also supports the creep experiments for the 1/1 film shown in Figure 8. The γ relaxation, associated with the local chain in the amorphous phase, was observed at around −130 °C. This magnitude of the dispersion peak became higher with increasing the EMMA content, which is in accordance with a decrease in the crystalline phase by introducing EMMA.

To clarify the mechanical dispersions of the blend films, positron annihilation was adopted, since it is well-known that an increase in the free volume holes can be clearly estimated by positron annihilation.[23] Actually, positron annihilation is one of the useful techniques used to investigate the size of the intermolecular spaces and relaxation characteristics of amorphous chains.[24−30] It has been shown that the lifetime (τ_3) of o-Ps in the spaces reflects the size, as shown by the following equation.[23,31,32]

$$\tau_3 = 0.5\left[1 - \frac{R}{R+\delta R} + \sin\left\{\frac{2\pi R}{R+\delta R}\right\}\right]^{-1} \qquad (1)$$

where $\delta R = 1.656$ Å was obtained by fitting the positron annihilation data in porous materials of known hole size.[33] This equation shows that the longer is τ_3, the bigger is the hole size in a polymer solid.

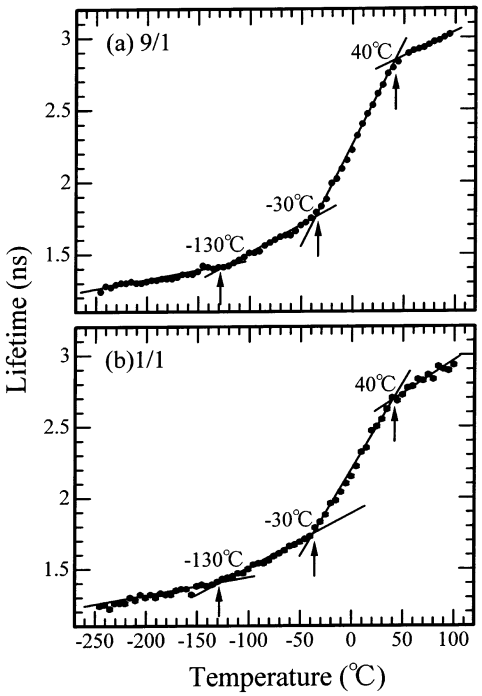

Figure 11. Lifetime (τ_3) of the long-lived component of Ps (orthopositronium, o-Ps) as a function of the temperature for the EMMA-III/UHMWPE = 9/1 and 1/1 films with $\lambda = 1$.

Figure 11 shows the variations of τ_3 of the 9/1 film and 1/1 film for the EMMA-III/UHMWPE system with $\lambda = 1$ as a function of the temperature. Since τ_3 is a good measure of the size of the intermolecular spaces, as shown by eq 1, the change in the increasing rate corresponds to the relaxation of the polymers, and above the relaxation temperature, the molecular motion and the expansion of intermolecular spaces easily occur. The first and second changes occur at about −130 and −30 °C, respectively, which correspond to the γ and β relaxations in Figure 10, respectively.

Figure 12 shows the transitions for the 9/1 and 1/1 films with $\lambda = 100$ observed for the EMMA-III/UHMWPE blends. Three transitions appeared at around −130 °C, −50 to −30 °C, and 38−40 °C, respectively. Comparing the three transitions of τ_3 with the mechanical dispersion peaks in Figure 10, it turns out that the β relaxation around −25 °C in Figure 10 corresponds to the second transition and the γ dispersion around −130 °C corresponds to the first transition. It is noteworthy that the β relaxation temperature of the 9/1 film became lower than that of the 1/1 film.

The good agreement between the transitions of τ_3 estimated by positron annihilation and mechanical dispersions by viscoelastic measurements indicates that the established concept of the β and γ dispersions for polyethylene are surely correct.[34] Namely, the γ dispersion corresponds to the local relaxation mode of polyethylene chains, and the β dispersion is the contribution from the motion of the amorphous chains. Therefore, positron annihilation is a useful tool to detect some weak motion of polymer groups and chains at low temperature.

The temperature dependence of τ_3 in Figure 12 is quite different from that observed for ultradrawn polyethylene films.[34] Namely, the second transition of τ_3 is clearly observed for 1/1 films with $\lambda = 100$, but not for

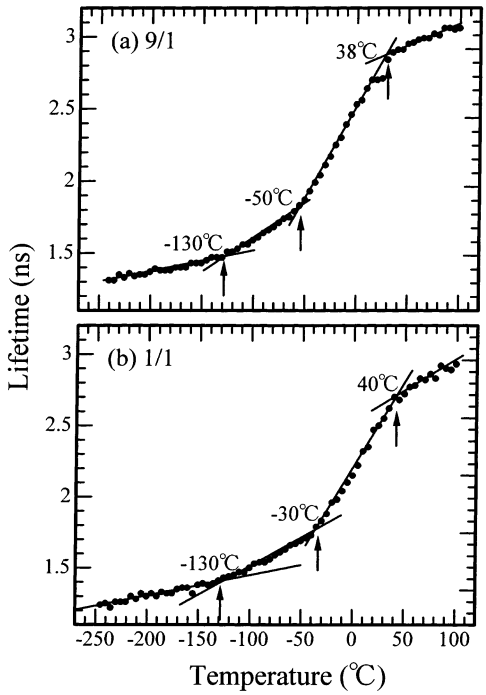

Figure 12. Lifetime (τ_3) of the long-lived component of Ps (orthopositronium, o-Ps) as a function of the temperature for the EMMA-III/UHMWPE = 9/1 and 1/1 composition films with $\lambda = 100$.

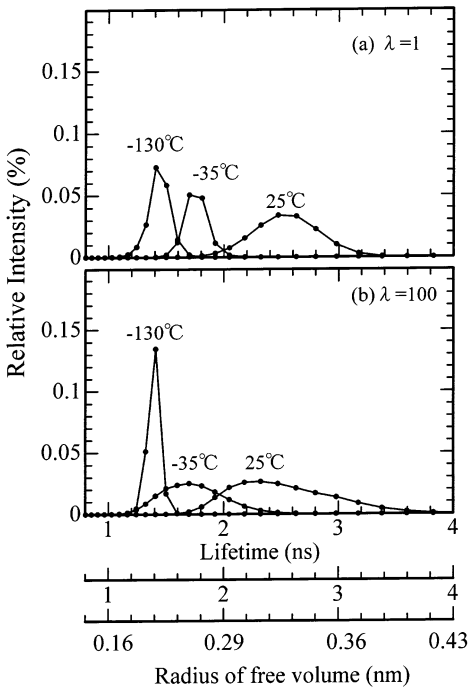

Figure 13. Histograms of the lifetime distribution of the EMMA-III/UHMWPE = 1/1 films at the indicated temperatures.

the corresponding UHMWPE. This is due to the difference in the mobility of the amorphous chains. Namely, the crystallinity of ultradrawn polyethylene ($\lambda = 100$) was higher than 90%. This justifies that the β relaxation also cannot be observed by using a dynamic mechanical measurement for ultradrawn polyethylene with $\lambda = 100$ (see Figures 9 and 10). This means that the mobility of highly oriented amorphous ethylene sequences of EMMA-III is quite different from that of oriented ethylene chains to form crystallites. This is in good agreement with those obtained by X-ray in Figure 5 and ^{13}C NMR in Figure 7. Incidentally, the same tendency was also observed for EMMA-II.

The third transition observed at 38−40 °C in Figures 11 and 12 is thought to be due to a partial melting of unstable small crystallites. Such a transition has never been observed for polyethylene homopolymer. This indicates that very small EMMA-III crystallites are much less stable than UHMWPE crystallites.

Parts a and b of Figure 13 show histograms of the o-Ps lifetime distributions at the indicated temperatures for the 1/1 films with $\lambda = 1$ and 100, respectively, observed for the EMMA-III/UHMWPE blends. The positron lifetime distributions were calculated by using the maximum entropy for a lifetime analysis (MELT).[35] The horizontal scale is also given as the radius of the mean free volume holes calculated by eq 1. The relative o-Ps intensities were calculated for the spectra measured at −130, −35, and 25 °C. It can be seen in Figure 13 that with increasing temperature the size distribution for the films with $\lambda = 1$ and 100 becomes broader and the peak position shifts to a larger value. This indicates that the free volumes within the 1/1 film become bigger and have a wider size distribution with increasing temperature and at the same moment the molecular motion becomes more active. The temperature dependence of the o-Ps lifetime distribution is due to thermal expansion of the intermolecular spaces of the specimen, which is related to an increase in the molecular mobility. It is of interest to consider that the free volume distribution becomes wider and wider as the temperature increases, and then the peak position at each temperature slightly shifts to a smaller scale with increasing the drawing ratio. The lifetime distribution of the drawn film ($\lambda = 100$) at 25 °C shows a much wider profile and larger holes, and the peak position slightly shifts to a shorter value compared with the film with $\lambda = 1$. These results showed that the average of the free volume holes in the 1/1 film tend to be slightly smaller with increasing λ, indicating a narrow distance between the highly oriented amorphous chains. Even at −35 °C around T_g of the 1/1 film, the free volume distribution at $\lambda = 100$ becomes wider than that at $\lambda = 1$.

Conclusion

Two kinds of EMMA with different contents of the MMA side group, EMMA-II or EMMA-III, were blended with UHMWPE by gelation/crystallization from solutions. The dry blend gels had the ability to form uniform films and could be elongated by more than 200-fold, even for the blend with a 90% EMMA content. The mechanism of ultradrawing was investigated by using DSC, WAXD, SAXS, ^{13}C solid-state NMR, and positron annihilation measurements. As a result, it was concluded that the drawing behavior depends on the EMMA contents. The greatest drawability for the 9/1 films was attributed to only highly orientation of UHMWPE crystallites, but most of the EMMA chains maintained a random orientation despite a preferential orientation of the UHMWPE chains with respect to the stretching direction. However, the ethylene sequences of EMMA chains within the 1/1 film were oriented together with the UHMWPE chains under the elongation process. Judging from the melting point of EMMA being much lower than that of UHMWPE, the highly orientated EMMA chains within the 1/1 film are thought to be due to cocrystallization from the effect of an epitaxial

nucleation surface of ethylene sequences of EMMA. From X-ray, ^{13}C NMR, and positron annihilation measurements, however, it was found that most of the oriented EMMA chains existed as an amorphous state. The preferential orientation of EMMA chains within the 1/1 films provided large values of the storage modulus (E') beyond 75 GPa at 20 °C, which were slightly lower than the value (100 GPa) of E' of UHMWPE films with $\lambda = 100$. In contrast, the values of E' of the 9/1 films with $\lambda = 100$ were 20−25 GPa. The temperature dependence of E'' of the 1/1 film with undrawn and drawn states was quite different from that of the corresponding UHMWPE homopolymer films. Namely, the β relaxation of the blends could be clearly observed because of the low crystallinity of the oriented EMMA main chains, while no peak was observed for the corresponding UHMWPE films. This phenomenon was in good agreement with the temperature dependence of the lifetime (τ_3) of the long-lived component of Ps (o-Ps).

Acknowledgment. EMMA specimens were furnished by Sumitomo Chemical Co. Ltd. The authors are indebted to Dr. Fujita in the company for his valuable comments for the specimens.

References and Notes

(1) Ma, L.; Bin, Y.; Sakai, Y.; Chen, Q.; Kurose, H.; Matsuo, M. *Macromolecules* **2001**, *34*, 4802.
(2) Ma, L.; Suzuki, T.; He, C.; Bin, Y.; Kurosu, H.; Matsuo, M. *Macromolecules* **2003**, *36*, 8056.
(3) Smith, P.; Lemstra, P. J.; Kalb, B.; Pennings, A. J. *Polym. Bull. (Berlin)* **1979**, *1*, 733.
(4) Smith, P.; Lemstra, P. J. *J. Mater. Sci.* **1980**, *15*, 505.
(5) Smith, P.; Lemstra, P. J.; Pipper, J. P. L.; Kiel, A. M. *Colloid Polym. Sci.* **1981**, *258*, 1070.
(6) Matsuo, M.; Sawatari, C. *Macromolecules* **1986**, *91*, 2036.
(7) Ogita, T.; Yamamoto, R.; Suzuki, N.; Ozaki, F.; Matsuo, M. *Polymer* **1991**, *32*, 822.
(8) Knittel, D.; Saus, W.; Schollmeyer, E. *Tech. Text.* **1995**, *38* 184.
(9) Bach, E.; Cleve, E.; Schollmeyer, E. J. *Text. Inst.* **1998**, *89*, 657.
(10) Sawatari, C.; Shimogiri, S.; Matsuo, M. *Macromolecules* **1987**, *20*, 1041.
(11) Sawatari, C.; Satoh, S.; Matsuo, M. *Polymer* **1990**, *32*, 1456.
(12) Matsuo, M.; Sawatari, C.; Ohhata, T. *Macromolecules* **1988**, *21*, 1317.
(13) Bin, Y.; Ma, L.; Adachi, L.; Kurose, H.; Matsuo, M. *Polymer* **2001**, *42*, 8125.
(14) Chen, Q.; Luo, H. J.; Yang, G.; Xu, D. F. *Polymer* **1997**, *38*, 1203.
(15) Shimizu, Y.; Harashina, Y.; Sugiura, Y.; Matsuo, M. *Macromolecules* **1995**, *28*, 6889.
(16) Ando, I.; Sorita, T.; Yamanobe, T.; Komoto, T.; Sato, H.; Deguchi, K.; Imanari, M. *Polymer* **1985**, *26*, 1864.
(17) Earl, W. L.; VanderHart, D. L. *Macromolecules* **1979**, *12*, 762.
(18) VanderHart, D. L. *J. Chem. Phys.* **1976**, *64*, 830.
(19) Matsuo, M.; Sawatari, C.; Nakano, T. *Polym. J.* **1986** *18*, 759.
(20) Sawatari, C.; Matsuo, M. *Macromolecules* **1989**, *22*, 2968.
(21) Khanna, Y. P.; Turi, E. A.; Taylor, T. J.; Vickroy, V. V.; Abott, R. F. *Macromolecules* **1985**, *18*, 1302.
(22) Kawai, H.; Suehiro, S.; Kyu, T.; Shimomura, A. *Polym. Eng. Rev.* **1983**, *3*, 10.
(23) Tao, S. J. *J. Phys. Chem.* **1972**, *56*, 5499.
(24) Walender, M.; Maurer, F. H. *J. Mater. Sci. Forum* **1992**, *105*, 1181.
(25) Suzuki, T.; Oki, Y.; Numajiri, M.; Miura, T.; Kondo, K.; Ito, Y. *Radiat. Phys. Chem.* **1995**, *45*, 657.
(26) Levey, B.; Lalovic, M.; Ache, H. J. *J. Chem. Phys.* **1989**, *90*, 3282.
(27) Zhang, Z.; Ito, Y. *Radiat. Phys. Chem.* **1991**, *38*, 221.
(28) Suzuki, T.; Oshima, N.; Miura, T.; Oki, Y.; Numajiri, M. *Polymer* **1997**, *37*, 5521.
(29) Uedono, A.; Kawano, T.; Tanigawa, S.; Ban, M.; Kyoto, M.; Uozumi, T. *J. Polym. Sci., Part B* **1997**, *35*, 1601.
(30) Van Krevelen, D. W.; Hoftyzer, P. J. *Properties of Polymers*; Elsevier Publications Co.: Amsterdam, 1976.
(31) Brandt, W.; Berko, S.; Walker, W. W. *Phys. Rev.* **1960**, *120*, 1289.
(32) Eldrup, M.; Lightbody, D.; Sherwood, J. N. *Chem. Phys.* **1981**, *63*, 51.
(33) Nakanishi, H.; Wang, S. J.; Jean, Y. C. In *Positron Annihilation Studies of Fluid*; Sharma, S. C., Ed.; World Scientific: Singapore, 1988; p 292.
(34) Matsuo, M.; Ma, L.; Azuma, M.; He, C.; Suzuki, T. *Macromolecules* **2002**, *35*, 3059.
(35) Shukla, A.; Hoffmann, L.; Manuel, A. A.; Peter, M. *Mater. Sci. Forum* **1997**, *255*, 233.

MA0305840